Testing the density matrix expansion against ab initio calculations of trapped neutron drops

S. K. Bogner, R. J. Furnstahl, H. Hergert, M. Kortelainen, P. Maris, M. Stoitsov, and J. P. Vary

Phys. Rev. C **84**, 044306 — Published 10 October 2011

DOI: 10.1103/PhysRevC.84.044306

Testing the density matrix expansion against ab initio calculations of trapped neutron drops

S.K. Bogner,[1] R.J. Furnstahl,[2] H. Hergert,[1] M. Kortelainen,[3] P. Maris,[4] M. Stoitsov,[3] and J.P. Vary[4]

[1]*National Superconducting Cyclotron Laboratory and Department of Physics and Astronomy, Michigan State University, East Lansing, MI 48824*
[2]*Department of Physics, Ohio State University, Columbus, OH 43210*
[3]*Department of Physics & Astronomy, University of Tennessee, Knoxville, Tennessee 37996*
Physics Division, Oak Ridge National Laboratory, Oak Ridge, Tennessee 37831
[4]*Department of Physics and Astronomy, Iowa State University, Ames, IA 50011*

Microscopic input to a universal nuclear energy density functional can be provided through the density matrix expansion (DME), which has recently been revived and improved. Several DME implementation strategies are tested for neutron drop systems in harmonic traps by comparing to Hartree-Fock (HF) and *ab initio* no-core full configuration (NCFC) calculations with a model interaction (Minnesota potential). The new DME with exact treatment of Hartree contributions is found to best reproduce HF results and supplementing the functional with fit Skyrme-like contact terms shows systematic improvement toward the full NCFC results.

PACS numbers: 21.10.-k,21.30.-x,21.60.Jz

I. INTRODUCTION

Experiments at radioactive ion beam facilities, studies of astrophysical systems such as neutron stars and supernovae, and nuclear energy and security needs have motivated multipronged efforts to develop nuclear energy density functionals (EDF's) with substantially reduced errors and improved predictive power away from stability. While great progress has been made in extending the reach of *ab initio* wave function methods beyond the lightest nuclei [1–4], the EDF approach remains the most computationally feasible method for a comprehensive description of medium and heavy nuclei [5]. However, the *ab initio* methods are vital tools for reaching the goal of robust functionals informed by microscopic internucleon interactions. As part of an ongoing program to achieve this goal, in this paper we investigate trapped neutron drops with a model interaction. In particular, EDF calculations using several density matrix expansion (DME) implementations are confronted with ab initio no-core full configuration (NCFC) [6] results.

The comparisons presented here exploit developments achieved within the Universal Nuclear Energy Density Functional (UNEDF) SciDAC-2 collaboration [7, 8]. The UNEDF project aims to develop a comprehensive theory of nuclear structure and reactions utilizing the most advanced computational resources and algorithms available, including high-performance computing techniques to scale to petaflop platforms and beyond [7]. One element of the UNEDF program involves the direct injection of microscopic physics into novel energy functionals, with the DME a key tool [9–12]. Another element has led to efficient density functional theory (DFT) solvers adapted for the DME [13] and to neutrons in external traps, which allow accurate and rapid testing of candidate functionals [14]. A third element is the extensive development of *ab initio* methods, including improved computational efficiencies [15] and extrapolation techniques for the NCFC [6] that allow exact calculations (with error bars) of the same neutron drop systems to which the functionals are applied.

Neutron drops are a powerful theoretical laboratory for improving existing nuclear energy functionals. Microscopic input to EDF's is particularly needed for neutron-rich nuclei, where there are fewer constraints from experiment. The properties of uniform neutron matter have been used in the past as a constraint on phenomenological functionals (e.g., see Refs. [16, 17]), but computational advances now allow accurate microscopic many-body calculations of inhomogeneous neutron drops in external potentials using quantum Monte Carlo or NCFC methods [18, 19]. These calculations can be used to identify deficiencies in existing functionals (e.g., of the Skyrme type as in Ref. [18]), to suggest or calibrate new versions, or simply to provide control data that supplements experiment for the optimization of functionals.

Neutron drops also provide favorable environments for the development and testing of non-empirical (i.e., microscopically based) functionals. The necessity of an external potential (because the untrapped system is unbound, with positive pressure) is turned into a virtue by allowing external control over the environment. Density Functional Theory (DFT), which provides the theoretical underpinning and computational framework for building a nuclear EDF, dictates that the same functional applies for any external potential, which can therefore be varied to probe and isolate different aspects of the EDF. In contrast, the treatment of self-bound systems (such as ordinary nuclei) has much less flexibility. Furthermore, there are serious complications from symmetry breaking [20], particularly for the relatively small systems where *ab initio* methods can also be applied.

The density matrix expansion was introduced long ago by Negele and Vautherin, who applied it to G-matrix effective interactions to derive a Skyrme-like Hartree-Fock

(HF) energy density functional. The DME has been revisited in recent years with the goal of applications to nuclear interactions sufficiently soft that many-body perturbation theory (MBPT) for nuclei is a quantitative framework. There are new formal DME developments, as well as new formulations that include hybrids between purely *ab initio* and phenomenological functionals. These must be tested and validated (or discarded if found to be inadequate); in general, due to the complexity of the various DME procedures and the involved density dependence they generate for the subsequent functional, we have no *a priori* guidance for the accuracy.

In this paper, we isolate the DME issues by using a simplified model interaction, the two-body Minnesota potential. Focusing on neutron drops is also advantageous because the self-consistent solution of a self-bound system magnifies approximation errors to the extent that it is difficult to analyze them. Of course, the main drawback of using neutron drops is the absence of control by experimental data. In our case this is not so relevant as we use a simple model interaction sufficient for conducting our basic tests of these methods. Our results here provide a foundation for testing more realistic interactions and improved functionals (e.g., that include pairing), and for extensions to self-bound nuclei.

In Section II, we briefly review the methods and inputs used. Results for the Minnesota potential are given in Section III for representative trap potentials and two closed-shell neutron drop systems. We summarize our observations and discuss the next steps to take in Section IV.

II. BACKGROUND

The present calculations combine ingredients from several parts of the UNEDF project. The technical details are described in full elsewhere, so we merely review the essential features.

A. DME

The density matrix expansion (DME) introduced by Negele and Vautherin [21, 22] provides a route to an EDF based on microscopic nuclear interactions through a quasi-local expansion of the energy in terms of various densities: $\rho(\mathbf{R})$, $\tau(\mathbf{R})$, $\nabla^2\rho(\mathbf{R})$, and so on. Kohn-Sham single-particle potentials are immediately obtained from simple functional derivatives with respect to these densities. The DME originated as an expansion of the Brueckner-Hartree-Fock energy constructed using the nucleon-nucleon G-matrix [21, 22], which was treated in a local (i.e., diagonal in coordinate representation) approximation.

The DME has been reformulated for spin-saturated nuclei using non-local low-momentum interactions in momentum representation [9], for which G-matrix summations are not needed because of the softening of the interaction. When applied to a Hartree-Fock energy functional, the DME yields an EDF in the form of a generalized Skyrme functional that is compatible with existing codes, by replacing Skyrme coefficients with density-dependent functions. As in the original application, a key feature of the DME is that it is not a pure short-distance expansion but includes resummations that treat long-range interactions correctly in a uniform system.

Extensions of the first calculations from Ref. [9] have modified the DME formalism from Negele and Vautherin [21], which provides an extremely poor description of the vector part of the density matrix [11]. The standard DME is much better at reproducing the scalar density matrices, but errors are still sufficiently large that the discrepancy with full finite-range Hartree-Fock calculations can reach the MeV per particle level. Gebremariam and collaborators [11] introduced a new phase space averaging (PSA) approach that accounts for the diffuse Fermi surface [23] and anisotropy [24] of the local momentum distribution, with no free parameters. The PSA treatment leads to substantial improvements, particularly for the vector density matrices, where relative errors in integrated quantities are reduced by as much as an order of magnitude across isotope chains [11]. In the present work, we test the difference between the original Negele-Vautherin (NV) and the new PSA prescriptions only for scalar parts.

The Fock energy exhibits spatial non-localities due to the convolution of finite-range interaction vertices with non-local density matrices. The DME factorizes the non-locality of the one-body density matrix by expanding it into a finite sum of terms that are separable in relative $\boldsymbol{r} \equiv \boldsymbol{r}_1 - \boldsymbol{r}_2$ and center of mass $\boldsymbol{R} \equiv (\boldsymbol{r}_1 + \boldsymbol{r}_2)/2$ coordinates. For example, in notation introduced in Refs. [11, 12], one expands the spin-scalar part (in both isospin channels) of the one-body density matrix as

$$\rho_t(\boldsymbol{r}_1, \boldsymbol{r}_2) \approx \sum_{n=0}^{n_{\max}} \Pi_n(kr)\ \mathcal{P}_n(\boldsymbol{R})\ , \tag{1}$$

where the functions $\{\mathcal{P}_n(\boldsymbol{R})\}$ denote various local densities and their gradients (through second order in the present work) and $\Pi_n(kr)$ denotes the so-called $\Pi-$functions, which depend on the particular formulation of the DME (here NV or PSA). The arbitrary momentum k sets the scale for the decay in the off-diagonal direction. As in Ref. [13], we will take k to be the local Fermi momentum related to the isoscalar density through

$$k \equiv k_F(\boldsymbol{R}) = \left(\frac{3\pi^2}{2}\rho_0(\boldsymbol{R})\right)^{1/3}\ , \tag{2}$$

although other choices are possible that include additional τ and $\Delta\rho$ dependencies [25].

It is possible to apply the DME to both Hartree and Fock energies so that the complete Hartree-Fock energy is mapped into a local functional. From the earliest

DME work, however, it was found that treating the Hartree contributions exactly provides a better reproduction of the density fluctuations and the energy produced from an exact HF calculation [22, 26]. Restricting the DME to the exchange contribution significantly reduces the self-consistent propagation of errors [22]. In addition, treating the Hartree contribution exactly does not complicate the numerical solutions of the resulting self-consistent equations compared to applying the DME to both Hartree and Fock terms. Here we will compare several prescriptions for handling the Hartree contribution, including a Taylor series expansion [27].

A consistent and systematic extension of the DME procedure beyond the Hartree-Fock level of MBPT has yet to be formulated. For now, attempts to microscopically construct a *quantitative* Skyrme-like EDF use some *ad hoc* approximations (e.g., using averaged rather than state-dependent energy denominators) when applying the DME to iterated contributions beyond the HF level and/or re-introduce some phenomenological parameters to be adjusted to data [21, 22, 28–30]. Recent work based on chiral NN and NNN effective field theory interactions motivates an approach to building upon the DME/HF functional that incorporates important microscopic physics while exploiting the highly developed Skyrme EDF technology [11–13].

The structure of the chiral interactions is such that each coupling in the DME/HF functional is decomposed into a density-independent coupling constant arising from zero-range contact interactions and a coupling function of the density arising from the universal long-range pion exchanges. This clean separation between long- and short-distance physics at the HF level suggests a semi-phenomenological approach where the long-distance couplings ($g_t^m(\mathbf{R}; V_\pi)$) are kept as is, and the zero-range constants C_t^m are optimized to finite nuclei and infinite nuclear matter properties [11, 12]. Thus,

$$g_t^{\rho\tau} \equiv g_t^{\rho\tau}(\mathbf{R}; V_\pi) + C_t^{\rho\tau}(V_{\rm ct}) \ , \tag{3}$$

and so on, so that the DME functional splits into two terms,

$$E[\rho] = E_{\rm ct}[\rho] + E_\pi[\rho] \ , \tag{4}$$

where the first term $E_{\rm ct}[\rho]$ collects all contributions from the contact part of the interaction plus higher-order short-range contributions encoded through the optimization to nuclei and nuclear matter, while the second term $E_\pi[\rho]$ collects the long-range NN and NNN pion exchange contributions at the Hartree-Fock level.

Because the contact contributions have essentially the same structure as those entering empirical Skyrme functionals, a microscopically guided Skyrme phenomenology has been suggested in which the contact terms in the DME functional are released for optimization to finite-density observables [11, 12]. This empirical procedure is supported by the observation that the dominant bulk correlations in nuclei and nuclear matter are primarily short-ranged in nature, as evidenced by Brueckner-Hartree-Fock (BHF) calculations where the Brueckner G-matrix "heals" to the free-space interaction at sufficiently large distances. One can loosely interpret the refit of the Skyrme constants to data as approximating the short-distance part of the G-matrix with a zero-range expansion through second order in gradients. In doing so, the constants can capture short-range correlation energy contributions beyond Hartree-Fock. We will test this strategy for incorporating BHF correlations from the Minnesota potential, with the free parameters of the volume part of the functional fixed to properties of infinite neutron matter and the free surface parameter adjusted to NCFC results. We will also consider a direct density-dependent modification to model BHF correlations.

B. Minnesota Potential

All of the calculations reported here use the Minnesota potential. This is a local NN-only potential that is the sum of three Gaussians in the radial coordinate r_{ij} [31]:

$$V_{ij} = [V_R + \frac{1}{2}(1+P_{ij}^\sigma)V_t + \frac{1}{2}(1-P_{ij}^\sigma)V_s]\frac{1}{2}(1+P_{ij}^r) \ , \tag{5}$$

where P^σ and P^r are spin and space exchange operators, respectively, and

$$V_R = V_{0R}e^{-\kappa_R r_{ij}^2} \ , \tag{6}$$

$$V_t = -V_{0t}e^{-\kappa_t r_{ij}^2} \ , \tag{7}$$

$$V_s = -V_{0s}e^{-\kappa_s r_{ij}^2} \ . \tag{8}$$

The parameters defining the V_{ij} are given in Table I. (Note: we have taken the exchange-mixture parameter u in Ref. [31] equal to be one.) The Minnesota potential reproduces NN effective range parameters and gives reasonable results for the binding energies of light nuclei. It is often used as a semi-realistic potential in model calculations.

TABLE I: Parameters defining the Minnesota potential, see Eqs. (5)–(8).

V_α	value	κ_α	value
V_{0R}	200.0 MeV	κ_R	1.487 fm^{-2}
V_{0t}	178.0 MeV	κ_t	0.639 fm^{-2}
V_{0s}	91.85 MeV	κ_s	0.465 fm^{-2}

For our purposes, the important characteristics of this potential are that it is local, which makes possible the immediate adaptation of current DME technology (which is not fully developed for non-local potentials), and that it is moderately soft, so that HF is a reasonable starting point and convergence is adequate in the NCFC. Because we plan to use low-momentum interactions in the future, this softness is consistent rather than a shortcoming of the model. While the Minnesota potential lacks important features of realistic interactions, such as tensor forces

and three-nucleon interactions, it provides a convenient, non-trivial test case for the DME that sets the stage for future tests.

C. EDF Solvers

The DME-based functionals described in the last section and in Ref. [13] have been implemented in the DFT solvers HFBRAD [32] and HFBTHO [33]. HFBRAD is a very fast solver for spherical nuclei and density-dependent local density approximations, while HFBTHO is much slower but calculates spherical and axially deformed nuclei, and can handle additional gradient corrections. A Fortran module for both solvers has been developed to implement the density-dependent parts of the EDF from the DME applied to chiral effective potentials [34]. The module contains all of the lengthy expressions for the DME couplings and their functional derivatives with respect to the density matrix, and for numerically stable approximations. The module also has the capability to calculate related infinite nuclear matter properties. We have developed a similar module that can handle expressions coming from the DME of the Minnesota potential plus external potentials. This module was linked to existing DFT solvers to calculate results presented here.

D. NCFC

To test the DME calculations, we use the *ab initio* no-core full configuration (NCFC) approach [6, 35] to provide exact results (with errors bars). The NCFC is closely related to the no-core shell model (NCSM) [36–39], as both employ a many-body harmonic oscillator basis that treats all nucleons as spectroscopically active. The basis space includes all many-body states with excitation quanta less than or equal to $N_{\max}$. A general feature is the possibility to completely remove spurious center-of-mass excitations, but the present application with an external potential does not exploit this capability. Rather, the center-of-mass motion is part of the physical system. The main difference between the NCFC and NCSM is that the NCSM employs an interaction renormalized to the finite many-body basis, such as the Lee-Suzuki effective interaction.

The NCFC approach involves the extrapolation of a sequence of finite matrix results with the bare interaction (as opposed to a Lee-Suzuki effective interaction) to the infinite basis space limit. This makes it possible to obtain basis-space-independent results for binding energies and other observables, and to evaluate their numerical uncertainties. The extrapolation methods are described in Ref. [6]. A recent calculation of ^{14}F in Ref. [4], made prior to the first experimental measurements, illustrates the predictive power of the NCFC approach when coupled with leadership class computer resources. Note that the present calculations do not exploit the full capabilities of the codes and computers available to further minimize theoretical errors, because current error bars are small enough for the present application.

To solve for ground-state energies, radii, and form factors of trapped neutron systems, the code MFDn [40–43] was generalized to allow for external potentials. Only spherically symmetric harmonic oscillator traps are used in the current investigation, but other shapes and deformed traps are also directly available.

III. RESULTS

The neutrons are confined by an external single-particle harmonic potential:

$$v_{\rm ext}(r) = \frac{1}{2} m\Omega^2 r^2 \ , \tag{9}$$

with harmonic oscillator parameter $\hbar\Omega$ varied from 5 MeV to 20 MeV. The calculations here use $N = 8$ and $N = 20$ neutrons, which form closed shells. In the future we will revisit this problem with pairing included and consider intermediate N values. Accurate NCFC results are limited to larger oscillator parameters because of slow convergence with $N_{\max}$ for the Minnesota potential. (Note: quantum Monte Carlo techniques such as GFMC or AFDMC are effective for smaller $\hbar\Omega$ and could be used for additional comparisons.) In some cases, extrapolations are not reliable and so only upper bounds to the total energy are given.

Comparisons between different DME treatments of the Hartree term are given in Tables II, III and IV. The full HF results provide a baseline for comparison of the Negele-Vautherin (HF/NV) and Phase-Space-Averaging (HF/PSA) approximations to HF, with variations based on how the Hartree part of the DME is treated. For each of the two DME implementations, there are three possibilities: treat Hartree with the same DME (NV or PSA), use a naive Taylor expansion (NT), or treat it exactly. We split the total energy into internal and trap contributions, with

$$E_{\rm int} = E_{\rm tot} - U_{\rm ext} \tag{10}$$

and

$$U_{\rm ext} = 4\pi \int dr\, r^2 v_{\rm ext}(r)\, \rho(r) \ . \tag{11}$$

Results are presented as deviations from the full HF results of the total and internal energies and the radii. These results are for spherical solutions, which were shown to minimize the energy. That is, by imposing a non-zero quadrupole moment as a constraint, we found in all cases that the total energy rapidly increases as the quadrupole moment deviates from zero.

It is evident that the DME with PSA and exact Hartree is systematically the closest to HF energies and radii. For

TABLE II: Comparison of DME approximations to HF total energies for different treatments of the Hartree term, expressed as deviations from the full Hartree-Fock results $\Delta E_i = E_i - E_{\rm HF}$ in MeV.

		HF/NV			HF/PSA		
N	$\hbar\Omega$	NV	NT	exact	PSA	NT	exact
8	3	0.1	0.2	0.1	0.0	0.1	0.0
8	5	0.4	0.8	0.4	−0.1	0.6	0.2
8	10	2.1	5.1	2.0	−1.7	4.1	0.9
8	15	4.2	12.9	4.6	−7.1	10.8	2.1
8	20	6.0	24.2	7.7		20.9	3.4
20	3	0.5	0.8	0.6	−0.1	0.4	0.2
20	5	1.8	3.4	2.3	−1.0	2.0	0.9
20	10	5.9	18.5	11.0	−14.0	12.0	3.9
20	15	3.8	44.3	22.7		31.6	7.9
20	20	−17.8	80.0	34.8		61.3	12.5

TABLE III: Comparison of DME approximations to HF internal energies for different treatments of the Hartree term, expressed as deviations from the full Hartree-Fock results $\Delta E_i = E_i - E_{\rm HF}$ in MeV.

		HF/NV			HF/PSA		
N	$\hbar\Omega$	NV	NT	exact	PSA	NT	exact
8	3	0.0	−0.0	0.0	0.1	0.0	0.1
8	5	−0.1	−0.4	−0.1	0.2	−0.3	−0.1
8	10	0.1	−1.0	−0.2	1.3	−1.0	−0.1
8	15	1.1	−1.5	0.3	5.4	−1.8	0.1
8	20	3.2	−1.9	1.1		−2.7	0.5
20	3	−0.2	−0.4	−0.3	0.1	−0.3	−0.1
20	5	−0.3	−1.2	−0.6	1.0	−0.8	−0.2
20	10	3.3	−2.2	0.3	11.9	−2.6	0.2
20	15	16.9	−2.0	4.4		−5.4	1.4
20	20	68.3	−1.2	11.1		−8.7	3.2

all DME approximations, internal energies are generally closer to full HF than the total energies. This can be understood because the internal energy comes mostly from the volume part of the EDF. DME and full HF agree for infinite (uniform) matter, so similar results can be expected from this part. However, one can see that the DME approximations give slightly larger radii, which implies slightly larger external energies, and so larger total energies. A possible explanation is that the DME coupling for the $\rho\Delta\rho$ term may not take into account all the surface effects.

Some of the DME/PSA entries in Tables II and IV are missing. In these cases, the calculation failed to converge because of EDF instabilities [44]. The instabilities occurred at high values of $\hbar\Omega$ when both the Hartree and Fock terms were taken from the DME. This could indicate some problems at high density in the Hartree part of the DME expressions. These instabilities are not, however, just simply related to the infinite neutron matter properties, and are therefore more involved [44].

An alternative to the DME for microscopically based EDF's uses the more completely microscopic but computationally far more intensive Optimized Effective Potential (OEP) method [10]. In Ref. [45], the OEP was applied to the same model problem of the Minnesota potential for neutrons in a trap. Comparisons made to exact HF results show that the exact exchange version of OEP is almost indistinguishable from HF, in contrast to the small but non-negligible discrepancies found here. Future comparisons as both methods continue to be refined will help to gauge the accuracy of DME approximations and guide the development of corrections.

TABLE IV: Comparison of DME approximations to HF rms radii for different treatments of the Hartree term, expressed as deviations from the full Hartree-Fock results $\Delta r_i = r_i - r_{\rm HF}$ in fm.

		HF/NV			HF/PSA		
N	$\hbar\Omega$	NV	NT	exact	PSA	NT	exact
8	3	0.01	0.02	0.00	−0.02	0.01	−0.01
8	5	0.03	0.07	0.03	−0.01	0.05	0.01
8	10	0.04	0.11	0.04	−0.06	0.09	0.02
8	15	0.03	0.14	0.04	−0.13	0.12	0.02
8	20	0.02	0.16	0.05		0.15	0.02
20	3	0.02	0.05	0.03	−0.02	0.02	0.01
20	5	0.04	0.09	0.06	−0.04	0.06	0.02
20	10	0.02	0.13	0.07	−0.18	0.09	0.02
20	15	−0.04	0.16	0.07		0.13	0.03
20	20	−0.20	0.18	0.05		0.15	0.02

To test schemes for incorporating correlations beyond HF, we use BHF calculations of neutron matter, which we expect to be quite accurate for the Minnesota potential. Two strategies are considered, following the discussion in Section II A.

The first strategy is based on the empirical observation that the ratio of the neutron matter HF and BHF results is a rather smooth function of density, which we denote $f(k_{\rm F})$. By assuming a rank-one separable expansion of the potential, $V(\mathbf{k},\mathbf{k}')$, the G-matrix would take the form $G(\mathbf{k},\mathbf{k}') \sim V(\mathbf{k},\mathbf{k}')/f(k_{\rm F})$ and then taking a simple Gaussian for the potential form factor and expanding out the integral that appears in the definition of $f(k_{\rm F})$, one motivates the form

$$f = a + b\rho^{1/3} + c\rho + d\rho^{5/3} + \dots \ . \tag{12}$$

The coefficient a, b, c, and d are determined by a fit. (Calculations omitting d were also made and yield similar results except for the densest neutron drops.) This strategy is implemented in the DFT solvers by evaluating the ρ dependence in the Fock terms as $\rho \to \rho(R)$, which means the DME/HF couplings simply get scaled by $f(\rho)$. In the exact Hartree treatment, the prescription $\rho \to 1/2[\rho(r_1)+\rho(r_2)]$ is used and otherwise $\rho(R)$ is used. This approach is labeled BHF/PSA (or just BHF) in the subsequent tables and figures (only results based on exact-Hartree, DME/PSA are given).

The second strategy follows Ref. [13] to incorporate BHF correlations by adding a contact part to the HF functional for the Minnesota potential. In general, the contact part $E_{\rm ct}[\rho]$ of the EDF has the form of the stan-

dard Skyrme functional

$$\mathcal{H}_{\rm ct}(\boldsymbol{r}) = \frac{\hbar^2}{2m}\tau_0 + \mathcal{H}_0^{\rm ct}(\boldsymbol{r}) + \mathcal{H}_1^{\rm ct}(\boldsymbol{r}) \,, \tag{13}$$

where

$$\begin{aligned}\mathcal{H}_t^{\rm ct}(\boldsymbol{r}) \;=\; & \left(C_{t0}^{\rho^2} + C_{tD}^{\rho^2}\rho_0^\gamma\right)\rho_t^2 + C_t^{\rho\tau}\rho_t\tau_t + C_t^{\rho\Delta\rho}\rho_t\Delta\rho_t \\ & + C_t^{\rho\nabla J}\rho_t\nabla J_t + C_t^{J^2}J_t^2 \,, \end{aligned} \tag{14}$$

and the isospin index $t = \{0,1\}$ labels isoscalar and isovector densities, respectively. In analogy to Ref. [13], the neutron coupling constants $C^i = C_0^i + C_1^i$, $i = \{\rho^2, \rho\tau\}$ are fitted to reproduce the neutron matter BHF results. This allows us to constrain the zero-range volume parameters of the DME-based functional, but not the parameters entering the surface part of the functional.

We optimize the surface parameters in the DME functional in a manner similar to the optimization done for standard Skyrme functionals. One could think of procedures based on semi-infinite neutron properties, or on the leptodermous expansion of the functional [46]. Here we optimize the surface coupling constant $C^{\rho\Delta\rho} = C_0^{\rho\Delta\rho} + C_1^{\rho\Delta\rho}$ to NCFC $E_{\rm tot}$ values presented in Tables V and VI by using theoretical error bars as weights. A simple minimization of the root-mean-square deviation yields almost the same result. The values for the neutron parameters of the Minnesota model are:

$$\begin{aligned} & C^{\rho^2} = -18.25\,\text{MeV fm}^3 \,, \quad C^{\rho\tau} = 4.57\,\text{MeV fm}^5 \,, \\ & C^{\rho\Delta\rho} = -1.8\,\text{MeV fm}^5 \,, \end{aligned} \tag{15}$$

with $C_D^{\rho^2} = C^{\rho\nabla J} = C^{J^2} = 0$. Calculations done with these parameters are labeled as "fit/PSA" in Tables V and VI and "fit" in the figures.

We have set the coupling constant $C_D^{\rho^2}$ to zero in the fit to neutron matter properties. In the usual Skyrme-DFT scheme, the density dependence controlled by the power γ is needed to produce reasonable saturation properties. For example, the incompressibility of symmetric nuclear matter is strongly affected by γ, and usually an acceptable value requires $\gamma < 1$. In the present calculations we do not constrain symmetric matter; indeed, the Minnesota potential does not produce realistic saturation. More generally, the density dependence from nonzero $C_D^{\rho^2}$ is used to effectively account for beyond-HF and three-body effects. The simplicity of the NN-only Minnesota potential seemingly lets us transfer beyond-HF effects to the other coupling constants and omit the $C_D^{\rho^2}$ term entirely.

In Tables V and VI, we summarize results for different trap parameters from the NV and PSA DME implementations of HF with exact Hartree, the two strategies to go beyond HF (BHF and fit, both based on PSA with exact Hartree), along with full HF and NCFC results. As already observed from the earlier tables, the comparisons to HF shows that the DME-HF/NV and DME-HF/PSA

TABLE V: Results for calculations of 8 neutron drops in harmonic potentials. All energies are in MeV and the rms radii $r_{\rm rms}$ are in fm. The NCFC results use up to the $N_{\rm max}$ in square brackets and parenthesis indicate the extrapolation uncertainty in the last quoted digit(s). The approximations are explained in the text.

Approx.	$\hbar\Omega$	$E_{\rm tot}$	$E_{\rm int}$	$U_{\rm ext}$	$r_{\rm rms}$
HF	5	71.9	37.6	34.3	3.78
HF/NV	5	72.3	37.5	34.8	3.80
HF/PSA	5	72.1	37.5	34.5	3.78
BHF/PSA	5	68.8	34.9	33.9	3.75
fit/PSA	5	70.0	36.8	33.2	3.71
NCFC [14]	5	< 69.5			
HF	10	142.4	69.6	72.8	2.75
HF/NV	10	144.5	69.5	75.0	2.79
HF/PSA	10	143.4	69.6	73.8	2.77
BHF/PSA	10	139.4	66.2	73.2	2.75
fit/PSA	10	138.6	67.3	71.3	2.72
NCFC [16]	10	138.1(6)	66(2)	72(2)	2.73(3)
HF	15	217.4	101.8	115.6	2.31
HF/NV	15	222.1	102.1	120.0	2.35
HF/PSA	15	219.5	101.9	117.6	2.33
BHF/PSA	15	214.8	98.5	116.2	2.31
fit/PSA	15	212.5	98.1	114.4	2.30
NCFC [16]	15	212.7(2)	98.6(4)	114.1(4)	2.293(4)
HF	20	296.4	135.1	161.3	2.04
HF/NV	20	304.1	136.3	167.8	2.09
HF/PSA	20	299.8	135.6	164.2	2.06
BHF/PSA	20	294.1	131.8	162.4	2.05
fit/PSA	20	290.9	130.0	160.9	2.04
NCFC [16]	20	290.8(2)	131.5(3)	159.3(3)	2.032(2)

TABLE VI: Results for calculations of 20 neutron drops in harmonic potentials with the same conventions as Table V.

Approx.	$\hbar\Omega$	$E_{\rm tot}$	$E_{\rm int}$	$U_{\rm ext}$	$r_{\rm rms}$
HF	5	230.4	120.9	109.6	4.26
HF/NV	5	232.8	120.2	112.5	4.32
HF/PSA	5	231.3	120.7	110.6	4.28
BHF/PSA	5	221.3	112.4	108.9	4.25
fit/PSA	5	223.0	117.5	105.5	4.18
HF	10	455.4	224.0	231.5	3.10
HF/NV	10	466.5	224.2	242.2	3.17
HF/PSA	10	459.3	224.1	235.2	3.12
BHF/PSA	10	445.0	215.7	229.3	3.08
fit/PSA	10	441.5	214.8	226.7	3.07
NCFC [8]	10	$< 452.$			
HF	15	693.0	328.1	364.9	2.59
HF/NV	15	715.7	332.5	383.2	2.66
HF/PSA	15	700.9	329.5	371.4	2.62
BHF/PSA	15	680.1	318.2	361.8	2.58
fit/PSA	15	675.9	313.2	362.7	2.59
NCFC [8]	15	678(8)	322(10)	356(10)	2.56(4)
HF	20	941.3	435.2	506.1	2.29
HF/NV	20	976.1	446.3	529.8	2.34
HF/PSA	20	953.7	438.4	515.4	2.31
BHF/PSA	20	928.1	417.7	510.4	2.30
fit/PSA	20	924.4	414.5	509.9	2.30
NCFC [8]	20	922(6)	425(10)	497(10)	2.27(3)

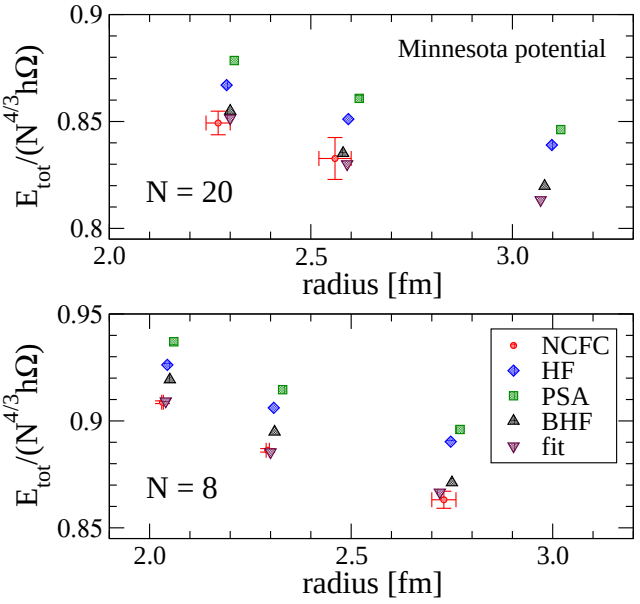

FIG. 1: (color online) Total energy and radius for 8 and 20 neutrons in a harmonic potential with oscillator parameters 10 MeV, 15 MeV and 20 MeV. Calculations using the NCFC are compared to full HF, the DME/PSA approximation to HF with exact Hartree, and results incorporating the resummed ladders for neutron matter using a density-dependent adjustment (BHF) and using fit coefficients from Eq. (15).

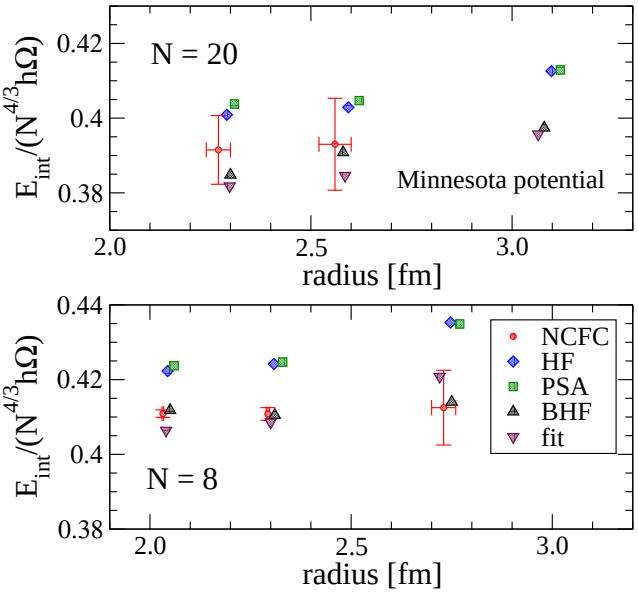

FIG. 2: (color online) Internal energy and radius for 8 and 20 neutrons in a harmonic potential with oscillator parameters 10 MeV, 15 MeV and 20 MeV as in Fig. 1.

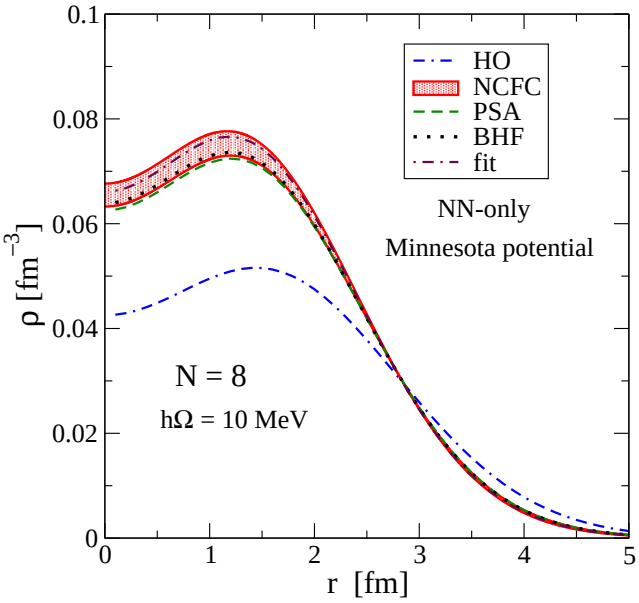

FIG. 3: (color online) Density for 8 neutrons in a harmonic potential with oscillator parameter 10 MeV. The non-interacting density (HO) is compared to calculations using the NCFC (shaded region), the DME/PSA approximation to HF with exact Hartree, and results incorporating the resummed ladders for neutron matter via a density-dependent adjustment (DME/PSA BHF) and using fit coefficients.

calculations have consistently higher energies and radii. These trends and the comparison to the NCFC results are evident in Figs. 1 and 2, where energies and radii from the various DME prescriptions are compared to a full Hartree-Fock calculation and to NCFC calculations for 8 and 20 neutrons. The energies have been scaled by the Thomas-Fermi energy trend $N^{4/3}\hbar\Omega$ [18] to remove the dominant dependence on N and $\hbar\Omega$. The error bars from the NCFC are from the extrapolations; the exact results for the Minnesota Hamiltonian are expected to lie within these error ranges.

The DME/PSA BHF results improve on the HF and DME/PSA HF results systematically for both the total and internal energies, and for the radii. They are within the errors of the NCFC in many cases. The DME/PSA fit result with only additional volume terms fit to neutron matter, is consistently worse than the HF results, particularly for the internal energy (not shown). This failure is consistent with Ref. [13], where the analogous prescription was found to introduce unacceptably large over-binding in nuclei. Here, the total energies and rms radii are systematically too small. But once a surface term is added and fit to the NCFC results for the total energies, excellent systematics are found for these energies and the predicted radii. The predicted internal energies are also improved although there are much larger differences from the central NCFC values than for the total energies.

The reproduction of coordinate-space densities and the corresponding momentum-space form factor are shown for some representative cases in Figs. 3, 4, and 5. These examples illustrate the very large range in interior density probed by this set of external potentials. The improvements noted for DMA/PSA BHF energies and radii are

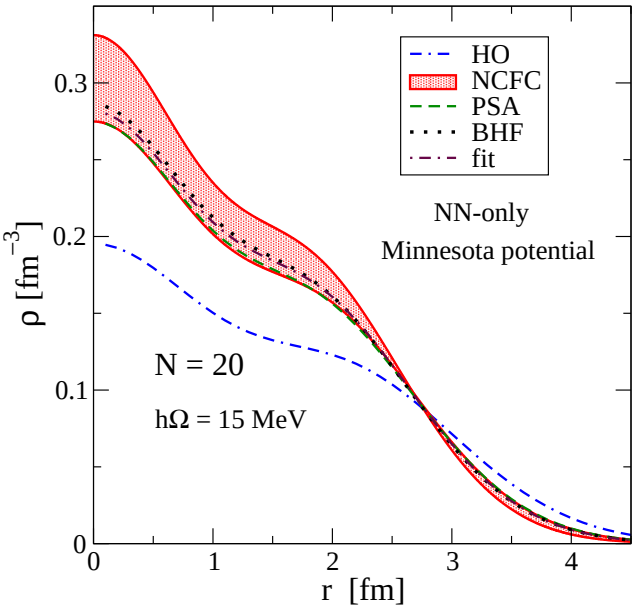

FIG. 4: (color online) Density for 20 neutrons in a harmonic potential with oscillator parameter 15 MeV, see Fig. 3 caption.

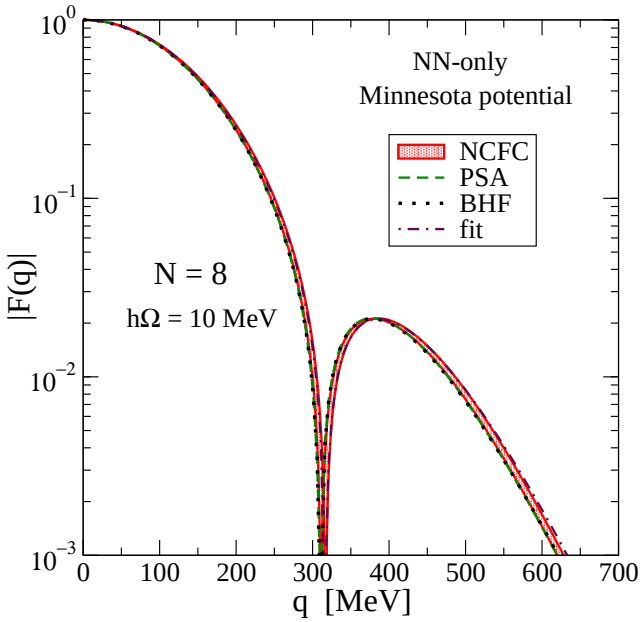

FIG. 5: (color online) Form factor for 8 neutrons in a harmonic potential with oscillator parameter 10 MeV, see Fig. 3 caption.

also seen for the densities. The DME/PSA fit results might be judged the best, although the error bands from the NCFC calculation are too large to allow a definitive conclusion. The form factor is given by:

$$F(q) = \frac{1}{N}\int dr\, 4\pi r^2 \rho(r) \frac{\sin qr}{qr} \ . \qquad (16)$$

Not surprisingly, the characteristic features of the first minimum and height of the second maximum are well reproduced within the NCFC error band.

IV. SUMMARY

In this paper, we perform test calculations to help develop density functionals for nuclei using microscopic input. In particular, we use the density matrix expansion (DME) as a bridge from many-body perturbation theory to EDF's that can be used in solvers and with optimization techniques developed for phenomenological Skyrme functionals. There are many implementation questions and options for the DME, some of which are addressed in the present work. Ultimately we will use high-precision two- and three-body nuclear interactions, such as from chiral effective field theory, evolved to softer forms using renormalization group methods. This softening makes them suitable for a MBPT treatment, unlike conventional interactions. As an interim step, we have used the Minnesota potential as a (moderately) soft, semi-realistic interaction for our tests.

The test environment is interacting neutrons in a harmonic trap. By varying the oscillator frequency of the trap, different inhomogeneous density profiles are probed. According to DFT, an EDF for self-bound nuclei should be the same for the neutron systems, with the simple addition of the external potential to the Kohn-Sham potential and $U_{\rm ext}$ to the energy functional. Thus we can make controlled explorations of the energies for different density distributions. The predictions are validated against *ab initio* calculations using NCFC methods, made possible for 8 and 20 neutrons by computational and algorithmic advances enabled by the UNEDF project. A key feature is that the same Hamiltonian is used for the *ab initio* solution and the functional. This allows us to more reliably isolate different sources of approximation errors.

Comparisons were first made between the DME at the HF level and full HF calculations. The best results for the improved form of the DME, which uses phase-space averaging (PSA), were consistently superior to the original Negele-Vautherin formulation. This agrees with the findings in Ref. [27], where it was found in non-self-consistent calculations of nuclei that the PSA-DME was the most accurate formulation when the expansion is truncated at second order in gradients. (Note: the improvement will be more significant for more realistic interactions including spin-orbit and tensor forces.) Several options for treating the Hartree (direct) contribution were considered, with a clear preference for an exact treatment in the PSA version of DME. This is consistent with past experience applying the DME.

There are still systematic discrepancies between the best DME Hartree-Fock calculations and the full HF results. This is in contrast to results from recent exact-exchange orbital-based calculations, which find extremely close agreement with HF for the same neutron systems and interactions [45]. Thus the source of the discrepancies seems to be the DME approximation and

not simply the use of a local Kohn-Sham potential. This implies that DME-based functionals will always need to be supplemented with some correction mechanism for inherent DME approximations as well as for errors from many-body approximations.

Hartree-Fock is a good quantitative starting point for these neutron drop systems with the Minnesota potential, but the full NCFC solutions show clear differences in the patterns of energies and radii. These differences are used as a testbed for two ways to incorporate correlations beyond HF in the DME functional. In both cases, Brueckner-Hartree-Fock (BHF) calculations of neutron matter with the Minnesota potential were used as the exact reference. (Instead, one could use *ab initio* calculations if available, or else calibrate to phenomenological values.)

In the first approach, the functional was modified by density-dependent terms, while in the second approach, the interaction was supplemented with Skyrme-like contact terms, whose coefficients were fit to the neutron matter calculation. The first method (labeled BHF in the figures), showed systematic improvement from DME Hartree-Fock toward the full NCFC results, both for the energies and the radius. The second method with volume terms only was found to be unacceptable, but the addition of a fit surface term improved the systematics dramatically, to roughly the error limits of the current NCFC calculations for the total energies and the predicted radii. These results validate the strategies planned for more realistic forces.

There are many ways forward from the present calculations. The neutron drop system will continue to be a valuable tool for diagnostic testing, which will include using non-harmonic (e.g., Woods-Saxon) and deformed traps. On-going development of the density matrix expansion includes the extension to pairing, which will be tested using open-shell neutron numbers, and extensions to incorporate higher-order MBPT and more complete low-momentum potentials. These extensions will be tested both in the neutron drop systems and for ordinary self-bound nuclei. Work in these directions is in progress.

Acknowledgments

We thank J. Drut and L. Platter for useful discussions. This work was supported by the Office of Nuclear Physics, U.S. Department of Energy under Contract Nos. DE-FC02-09ER41583 and DE-FC02-09ER41582 (UNEDF SciDAC Collaboration), DE-FG02-96ER40963 and DE-FG02-07ER41529 (University of Tennessee), DE-FG0587ER40361 (Joint Institute for Heavy Ion Research), DE-FC02-09ER41581, DE-FG02-87ER40371 and DE-FC02-09ER41585. Computational resources were provided by the National Center for Computational Sciences (NCCS) and the National Institute for Computational Sciences (NICS) at Oak Ridge National Laboratory through the INCITE program. Additional computational resources were provided by the National Energy Research Scientific Computing Center (NERSC) at Lawrence Berkeley National Laboratory.

[1] S. C. Pieper, Nucl. Phys. A **751**, 516 (2005), nucl-th/0410115.
[2] S. Quaglioni and P. Navratil, Few Body Syst. **44**, 337 (2008), 0712.0855.
[3] G. Hagen, T. Papenbrock, D. J. Dean, and M. Hjorth-Jensen, Phys. Rev. Lett. **101**, 092502 (2008), 0806.3478.
[4] P. Maris, A. M. Shirokov, and J. P. Vary, Phys. Rev. **C81**, 021301 (2010), 0911.2281.
[5] M. Bender, P.-H. Heenen, and P.-G. Reinhard, Rev. Mod. Phys. **75**, 121 (2003).
[6] P. Maris, J. P. Vary, and A. M. Shirokov, Phys. Rev. C **79**, 014308 (2009), 0808.3420.
[7] G. F. Bertsch, D. J. Dean, and W. Nazarewicz, SciDAC Review **6**, 42 (2007).
[8] For more details, see: `http://unedf.org`.
[9] S. K. Bogner, R. J. Furnstahl, and L. Platter, Eur. Phys. J. A **39**, 219 (2009), 0811.4198.
[10] J. E. Drut, R. J. Furnstahl, and L. Platter, Prog. Part. Nucl. Phys. **64**, 120 (2010), 0906.1463.
[11] B. Gebremariam, T. Duguet, and S. K. Bogner, Phys. Rev. **C82**, 014305 (2010), 0910.4979.
[12] B. Gebremariam, S. K. Bogner, and T. Duguet, Nucl. Phys. **A851**, 17 (2011), 1003.5210.
[13] M. Stoitsov et al., Phys. Rev. **C82**, 054307 (2010), 1009.3452.
[14] M. Kortelainen et al., Phys. Rev. **C82**, 024313 (2010), 1005.5145.
[15] P. Maris, M. Sosonkina, J. P. Vary, E. G. Ng, and C. Yang, Proc. Comp. Sci. **1**, 97 (2010).
[16] E. Chabanat, J. Meyer, P. Bonche, R. Schaeffer, and P. Haensel, Nucl. Phys. **A627**, 710 (1997).
[17] B. A. Brown, Phys. Rev. **C58**, 220 (1998).
[18] S. Gandolfi, J. Carlson, and S. C. Pieper, Phys. Rev. Lett. **106**, 012501 (2011), 1010.4583.
[19] J. Carlson, S. Gandolfi, P. Maris, J. Vary, and S. Pieper (2011), in preparation.
[20] T. Duguet and J. Sadoudi, J. Phys. **G37**, 064009 (2010), 1001.0673.
[21] J. W. Negele and D. Vautherin, Phys. Rev. C **5**, 1472 (1972).
[22] J. W. Negele and D. Vautherin, Phys. Rev. C **11**, 1031 (1975).
[23] M. Durand, V. S. Ramamurthy, and P. Schuck, Phys. Lett. B **113**, 116 (1982).
[24] A. Bulgac and J. M. Thompson, Phys. Lett. B **383**, 127 (1996).
[25] X. Campi and A. Bouyssy, Phys. Lett. B **73**, 263 (1978).
[26] D. Sprung, M. Vallieres, X. Campi, and C.-M. Ko, Nucl. Phys. A **253**, 1 (1975).
[27] B. G. Carlsson and J. Dobaczewski, Phys. Rev. Lett. **105**,

122501 (2010), 1003.2543.
[28] F. Hofmann and H. Lenske, Phys. Rev. **C57**, 2281 (1998), nucl-th/9705049.
[29] N. Kaiser, S. Fritsch, and W. Weise, Nucl. Phys. A **724**, 47 (2003), nucl-th/0212049.
[30] N. Kaiser and W. Weise, Nucl. Phys. **A836**, 256 (2010), 0912.3207.
[31] D. R. Thompson, M. Lemere, and Y. C. Tang, Nucl. Phys. **A286**, 53 (1977).
[32] K. Bennaceur and J. Dobaczewski, Comput. Phys. Commun. **168**, 96 (2005), nucl-th/0501002.
[33] M. V. Stoitsov, J. Dobaczewski, W. Nazarewicz, and P. Ring, Comput. Phys. Commun. **167**, 43 (2005), nucl-th/0406075.
[34] M. Kortelainen and M. Stoitsov (2011), to be published.
[35] S. K. Bogner et al., Nucl. Phys. A **801**, 21 (2008), 0708.3754.
[36] D. C. Zheng, J. P. Vary, and B. R. Barrett, Phys. Rev. **C50**, 2841 (1994), nucl-th/9405018.
[37] D. C. Zheng, B. R. Barrett, J. P. Vary, W. C. Haxton, and C. L. Song, Phys. Rev. **C52**, 2488 (1995).
[38] P. Navratil, J. P. Vary, and B. R. Barrett, Phys. Rev. Lett. **84**, 5728 (2000), nucl-th/0004058.
[39] P. Navratil, J. P. Vary, and B. R. Barrett, Phys. Rev. C **62**, 054311 (2000).
[40] J. Vary, *The Many-Fermion-Dynamics Shell-Model Code* (Iowa Sate University, 1992 (unpublished)).
[41] P. Sternberg, E. G. Ng, C. Yang, P. Maris, J. P. Vary, M. Sosonkina, and H. V. Le (2008), in Proceedings of the 2008 ACM/IEEE Conference on Supercomputing, Austin, Texas, 2008 (IEEE, New York, 2008).
[42] J. P. Vary, P. Maris, E. Ng, C. Yang, and M. Sosonkina, J. Phys. Conf. Ser. **180**, 012083 (2009), 0907.0209.
[43] P. Maris, M. Sosonkina, J. P. Vary, E. G. Ng, and C. Yang, Procedia Comp. Sci. **1**, 97 (2010).
[44] M. Kortelainen and T. Lesinski, J. Phys. **G37**, 064039 (2010), 1002.1321.
[45] J. E. Drut and L. Platter (2011), 1104.4357.
[46] P.-G. Reinhard, M. Bender, W. Nazarewicz, and T. Vertse, Phys.Rev. **C73**, 014309 (2006), nucl-th/0510039.